

## PAPER

# Treatment of boundary conditions by finite difference time domain method

Hisaharu Suzuki<sup>\*</sup>, Akira Omoto<sup>†</sup> and Kyoji Fujiwara<sup>‡</sup>

*Faculty of Design, Kyushu University,  
Shiobaru 4-9-1, Minamiku, Fukuoka, 815-8540 Japan*

*(Received 1 January 2006, Accepted for publication 20 June 2006)*

**Abstract:** In this paper, we propose a simple method that considers boundary conditions in a finite difference time domain (FDTD) scheme by varying density, sound speed and flow resistance. A method based on a Rayleigh model is also proposed, and by these methods, we can design the frequency characteristics of normal incident absorption coefficient arbitrarily. These methods have three advantages: 1. easy coding, 2. easy designing of a frequency characteristic of normal incident absorption coefficient and 3. easy configuration of material thickness. For example, by our method, we can simulate the sound field in a reverberation chamber with a thick material such as glass wool. To confirm the accuracy of the model used, we compare the normal incident absorption coefficient with a one-dimensional exact solution. Results show that the model is sufficiently accurate. Although our method requires a high cost for calculation power and memory, a practical increase in elapsed time can be ignored. This method provides an easy way of analyzing the inner region of a material.

**Keywords:** FDTD, Surface impedance, Rayleigh model

**PACS number:** 43.55.Ka [doi:10.1250/ast.28.16]

## 1. INTRODUCTION

In most finite difference time domain (FDTD) methods in acoustics, the ‘surface impedance model’ is used to examine boundary conditions. In this paper, we propose an alternative method in which a material is modeled on the basis of density, sound speed, and flow resistance using a Staggered-Grid mesh [1,2]. By setting these three parameters on each grid, a difference in characteristic impedance is proposed, and simultaneously, they are recognized as boundary conditions. This is a very simple and primitive way of creating arbitrary boundary conditions.

Surface impedance is widely used as a boundary condition in numerical acoustic simulation. This is also true in an FDTD method, and several surface impedance models were proposed, for example, in [1,2]. In previous models, surface impedance is expressed as coefficients that are set between the sound pressure and particle velocity grids in the  $x$ ,  $y$  and  $z$  directions.

In particular, in the method developed by Chiba and Kashiwa [1], surface impedance is modeled by an RCL equivalent circuit, and this model makes it possible to design frequency characteristics. In these methods, surface

impedance can be directly considered, and the inner region of a material can be ignored. Therefore, they reduce the number of calculation grids, and require a lower CPU resource. On the other hand, intense coding effort is required for the normal vector direction of a boundary, particularly in the case of an arbitrary shape.

Typically, surface impedance is considered at the boundary of two mediums with different characteristic impedances. However, in the FDTD method, it is possible to set the medium properties on each calculation grid, and the set properties, such as density, sound speed, and flow resistance, can modify the characteristic impedance on the grid. A modified characteristic impedance yields surface impedance equivalently. As a result, it is possible to set up surface impedance in the FDTD simulation by modifying the characteristic impedance on the grid.

Two boundary models are assumed in this paper. The first model involves varying density and sound speed, and is coded more easily than an impedance vector model. The second model is a generally extended Rayleigh model [3,4], which makes it possible to simulate sound fields with a porous material of finite thickness.

Using the Rayleigh model, we can describe the porous materials, such as glass wool. It is a very simple model and is given by a continuous equation and an equation of motion with a flow resistance term. On the other hand, the Delany-Bazley [5] or Miki [6] model is a well-known

---

<sup>\*</sup>e-mail: hisaha@souldsp.jp

<sup>†</sup>e-mail: omoto@design.kyushu-u.ac.jp

<sup>‡</sup>e-mail: fujiwara@design.kyushu-u.ac.jp

model for porous materials. These models are expressed as frequency-domain functions, and are useful for steady-state analical methods, such as the boundary and finite element methods. These models are reliable and useful, because they are given by an experimental regression line. On the other hand, since a wave equation is directly digitized in the FDTD method, it is difficult to use the frequency domain model. This is the reason why the Rayleigh model is adopted here.

In this paper, first, the formulization of each model is explained. Secondly, the accuracy of normal incident sound absorption coefficient is explained by comparing it with a one-dimensional exact solution. Lastly, two-dimensional calculation examples of each model are shown, and the effectiveness of the proposed method is examined.

## 2. FORMULIZATION

### 2.1. Finite Difference Expressions of Equations

An equation of continuity of sound wave in air is given by

$$\frac{\partial p}{\partial t} + \kappa \left( \frac{\partial u_x}{\partial x} + \frac{\partial u_y}{\partial y} + \frac{\partial u_z}{\partial z} \right) = 0, \quad (1)$$

where  $p$  is the sound pressure,  $u_x$ ,  $u_y$  and  $u_z$  are the particle velocities in the  $x$ ,  $y$  and  $z$  directions, respectively, and  $\kappa$  is the bulk modulus of the medium. An equation of motion in the  $x$  direction is given by

$$\frac{\partial p}{\partial x} + \rho \frac{\partial u_x}{\partial t} = 0. \quad (2)$$

Sound pressure and particle velocities are discretized by placing a Staggered-Grid mesh. The finite difference version of the equation of continuity is expressed as

$$\begin{aligned} & p\left(i - \frac{1}{2}, j - \frac{1}{2}, k - \frac{1}{2}, n + \frac{1}{2}\right) \\ &= p\left(i - \frac{1}{2}, j - \frac{1}{2}, k - \frac{1}{2}, n - \frac{1}{2}\right) \\ & - \left[ \frac{\Delta t \kappa}{\Delta x} [u_x(i, j, k, n) - u_x(i - 1, j, k, n)] \right. \\ & + \frac{\Delta t \kappa}{\Delta y} [u_y(i, j, k, n) - u_y(i, j - 1, k, n)] \\ & \left. + \frac{\Delta t \kappa}{\Delta z} [u_z(i, j, k, n) - u_z(i, j, k - 1, n)] \right], \quad (3) \end{aligned}$$

and the discretized form of the equation of motion in the  $x$  direction is expressed as

$$\begin{aligned} & u_x(i, j, k, n + 1) = u_x(i, j, k, n) \\ & - \frac{\Delta t}{\Delta x \rho} \left[ p\left(i + \frac{1}{2}, j - \frac{1}{2}, k - \frac{1}{2}, n + \frac{1}{2}\right) \right. \\ & \left. - p\left(i - \frac{1}{2}, j - \frac{1}{2}, k - \frac{1}{2}, n + \frac{1}{2}\right) \right], \quad (4) \end{aligned}$$

where  $p(i, j, k, n)$  is the sound pressure on the grid of  $(i, j, k)$  at the time of  $n$  and  $u_x(i, j, k, n)$ ,  $u_y(i, j, k, n)$  and  $u_z(i, j, k, n)$  are the particle velocities in the  $x$ ,  $y$  and  $z$  directions, respectively.  $\Delta t$  is the sampling time, and  $\Delta x$ ,  $\Delta y$  and  $\Delta z$  are the grid widths in the  $x$ ,  $y$  and  $z$  directions, respectively. The sampling time is determined by sound speed and spacial grid width for stability [7]. For example, the Matlab source code in a two-dimensional finite difference equation is written as (in the example, the two-dimensional case is assumed for simplicity)

```
%equation of continuity
for i=1:I-1
    for j=1:J-1
        P2(i,j) = P1(i,j) ...
            -dt*K/dx*( Ux1(i+1,j)-Ux1(i,j) ) ...
            -dt*K/dy*( Uy1(i,j+1)-Uy1(i,j) );
    end
end

%equation of motion
for i=1:I-1
    for j=1:J-1
        Ux2(i+1,j) = Ux1(i+1,j) ...
            -dt/dx/rho*( P2(i+1,j)-P2(i,j) );
        Uy2(i,j+1) = Uy1(i,j+1) ...
            -dt/dy/rho*( P2(i,j+1)-P2(i,j) );
    end
end

%swapping matrix
tmp = P1; P1 = P2; P2 = tmp;
tmp = Ux1; Ux1 = Ux2; Ux2 = tmp;
tmp = Uy1; Uy1 = Uy2; Uy2 = tmp;
```

where P1 is the current variable of sound pressure and P2 is the updated variable of sound pressure. Ux1 and Uy1, and Ux2 and Uy2 are the current and updated variables of the particle velocities in the  $x$  and  $y$  directions, respectively.  $K$  is the bulk modulus constant, and  $\rho$  is the mass density constant.  $dx$  and  $dy$  are the variables of spacial grid width, and  $dt$  is the variable of sampling time.  $I$  and  $J$  are the variables of calculation field size. If the code is iterated, it can be monitored that P1, Ux1 and Uy1 vary momentarily.

### 2.2. Existing Model of Surface Impedance

The simplest surface impedance model is proposed in [2], in which the surface impedance  $Z$  is expressed as

$$Z = \frac{p}{u}, \quad (5)$$

where  $p$  is the sound pressure and  $u$  is the particle velocity. Figure 1 shows an example of an arrangement of grids at a

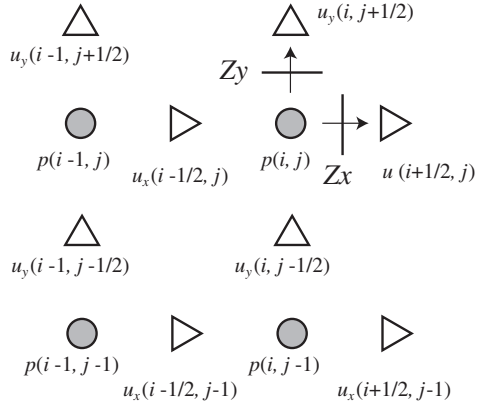


**Fig. 1** Layout of grids and impedance vector in previously used model.

two-dimensional sound field with impedance boundaries, and finite difference equations that update  $u_x(i + 1/2, j, n + 1)$  and  $u_y(i, j + 1/2, n + 1)$  are expressed as

$$u_x(i + 1/2, j, n + 1) = p(i, j, n + 1/2)/Z_x, \quad (6)$$

$$u_y(i, j + 1/2, n + 1) = p(i, j, n + 1/2)/Z_y. \quad (7)$$

$Z_x$  and  $Z_y$  are the impedances in the  $x$  and  $y$  directions, respectively. If the direction of surface impedance is outer, it is necessary that the spacial index of particle velocity, which is different from sound pressure indexes, must be incremented. By this method, we can avoid the calculation of iterating in the inner region of a boundary, and the CPU load can be lower. However, this method requires special judgment of directions for arbitrary boundary conditions. This indicates that more difficult programming is required in this method than in Method I presented in Sect. 2.3.

### 2.3. Method of Varying Sound Speed and Medium Density (Method I)

Figure 2 shows two mediums with different mass densities and sound speeds. These mediums also have different characteristic impedances. The densities are denoted  $\rho_1$  and  $\rho_2$ , the sound speeds,  $c_1$  and  $c_2$ , and characteristic impedances,  $Z_1 = \rho_1 c_1$  and  $Z_2 = \rho_2 c_2$ , respectively. The normal incident absorption coefficient  $\alpha_0$  is calculated as

$$\alpha_0 = 1 - \left| \frac{Z_2 - Z_1}{Z_2 + Z_1} \right|^2, \quad (8)$$

and the ratio of characteristic impedance  $a$  is

$$a = \frac{1 + \sqrt{1 - \alpha_0}}{1 - \sqrt{1 - \alpha_0}}. \quad (9)$$

If we set the medium property as  $\rho_2 = a\rho_1$  or  $c_2 = ac_1$ , the normal impedance can be set as having the desired normal incident absorption coefficient. In this method, the considered field shows the distribution of sound speed at each

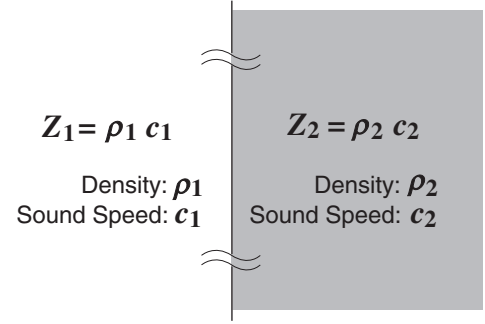


**Fig. 2** Two mediums with different characteristic impedances.

calculation grid. In the FDTD method, sampling frequency is determined by sound speed and spacial grid width for stability [7]. The maximum sound speed of the sound field must be used for the stability condition. The coding of this method is very easy, and the simplified Matlab code is as follows.

```
%equation of continuity
for i=1:I-1
    for j=1:J-1
        P2(i,j) = P1(i,j) ...
            -dt*K(i,j)/dx*( Ux1(i+1,j)-Ux1(i,j) ) ...
            -dt*K(i,j)/dy*( Uy1(i,j+1)-Uy1(i,j) );
    end
end

%equation of motion
for i=1:I-1
    for j=1:J-1
        Ux2(i+1,j) = Ux1(i+1,j) ...
            -dt/dx/rho(i,j)*( P2(i+1,j)-P2(i,j) );
        Uy2(i,j+1) = Uy1(i,j+1) ...
            -dt/dy/rho(i,j)*( P2(i,j+1)-P2(i,j) );
    end
end

%swapping matrix
tmp = P1; P1 = P2; P2 = tmp;
tmp = Ux1; Ux1 = Ux2; Ux2 = tmp;
tmp = Uy1; Uy1 = Uy2; Uy2 = tmp;
```

where  $\rho$  is the variable of mass density,  $K$  is the bulk modulus, and the other variables are the same as those in Sect. 2.1. The change in sound speed is included in the bulk modulus in this case.

### 2.4. Method Based on Rayleigh Model (Method II)

In the Rayleigh model [3,4], a porous material is replaced by a set of thin pipes with perfectly rigid bodies, as shown in Fig. 3. In this model, the equation of continuity

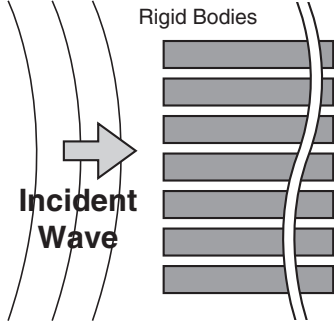


**Fig. 3** Image of Rayleigh model in which the set of thin pipes with rigid bodies are assumed.

in the porous material is the same as that in air and is given by

$$\frac{\partial p}{\partial t} + \kappa \left( \frac{\partial u_x}{\partial x} + \frac{\partial u_y}{\partial y} + \frac{\partial u_z}{\partial z} \right) = 0. \quad (10)$$

Here, we assume that air viscosity is dominant, and the distribution of air flow is constant in the thin pipes. This distribution is regarded as the constant flow distribution, and the equation of motion is described by adding a diffusion term in which particle velocity is multiplied by  $\sigma$ , which is flow resistance. Thus, the equation of motion in the  $x$  direction is expressed as

$$\frac{\partial p}{\partial x} + \rho \frac{\partial u_x}{\partial t} + \sigma u_x = 0. \quad (11)$$

Although excess attenuation is treated only in the  $x$  direction in the original Rayleigh model, the model can be extended to two- or three-dimensional cases straightforwardly. The expanded equation of motion is expressed as

$$\frac{\partial p}{\partial x} + \rho \frac{\partial u_x}{\partial t} + \sigma_x u_x = 0, \quad (12a)$$

$$\frac{\partial p}{\partial y} + \rho \frac{\partial u_y}{\partial t} + \sigma_y u_y = 0, \quad (12b)$$

$$\frac{\partial p}{\partial z} + \rho \frac{\partial u_z}{\partial t} + \sigma_z u_z = 0. \quad (12c)$$

Although the flow resistance of the material may depend on the directions,  $\sigma_x$  and  $\sigma_y$  are set to be identical in this paper for simplicity. Further discussion should be required to verify the accuracy of the method of introducing the angle dependence of flow resistance in the FDTD method.

The finite differential version in the  $x$  direction is expressed as

$$u_x(i, j, k, n+1) = \left( 1 - \frac{\Delta t \sigma_x}{\rho} \right) u_x(i, j, k, n)$$

$$- \frac{\Delta t}{\Delta x \rho} \left[ p \left( i + \frac{1}{2}, j - \frac{1}{2}, k - \frac{1}{2}, n + \frac{1}{2} \right) - p \left( i - \frac{1}{2}, j - \frac{1}{2}, k - \frac{1}{2}, n + \frac{1}{2} \right) \right]. \quad (13)$$

We must update Eqs. (3) and (13) in the inner region of the material. The difference from the original traveling case in air is the term of flow resistance in the  $x$ ,  $y$  and  $z$  directions. If we express the equation of motion in a two-dimensional field as the  $x$  and  $y$  terms in Eq. (12), the update equations are expressed as follows;

```
%equation of continuity
for i=1:I-1
    for j=1:J-1
        P2(i,j) = P1(i,j) ...
            -dt*K/dx*( Ux1(i+1,j)-Ux1(i,j) ) ...
            -dt*K/dy*( Uy1(i,j+1)-Uy1(i,j) );
    end
end

%equation of motion
for i=1:I-1
    for j=1:J-1
        Ux2(i,j)=(1-dt*sx(i,j)/rho)*Ux1(i,j) ...
            -dt/dx/rho*( P2(i+1,j)-P2(i,j) );
        Uy2(i,j)=(1-dt*sy(i,j)/rho)*Uy1(i,j) ...
            -dt/dy/rho*( P2(i,j+1)-P2(i,j) );
    end
end

%swapping matrix
tmp = P1; P1 = P2; P2 = tmp;
tmp = Ux1; Ux1 = Ux2; Ux2 = tmp;
tmp = Uy1; Uy1 = Uy2; Uy2 = tmp;
```

where  $sx(i,j)$  and  $sy(i,j)$  are the flow resistances in the  $x$  and  $y$  directions, respectively, and the other variables are the same as those in Sect. 2.1. If these resistances are equal to zero, there is no absorption by flow resistance, and the equation of motion corresponds to that in normal air. In this case, only setting the flow resistance makes it possible to analyze the sound field with an absorbing material of finite thickness.

### 3. EXAMINATION OF ACCURACY OF METHOD I

#### 3.1. Normal Incident Sound Absorption Coefficient

A one-dimensional pipe is assumed, as shown in Fig. 4, and the normal incident absorption coefficient is calculated by one-dimensional FDTD. The grid width is 0.0025 m, and the sampling frequency is set to be 388,060 Hz. The sampling frequency is determined by the constant multiple

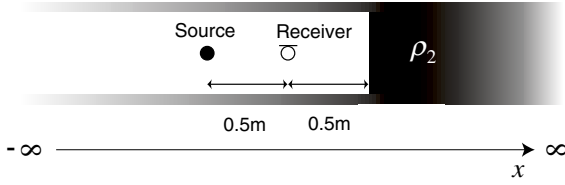


**Fig. 4** Image of one-dimensional sound field in which acoustic tube of infinite length and material of infinite thickness are assumed.

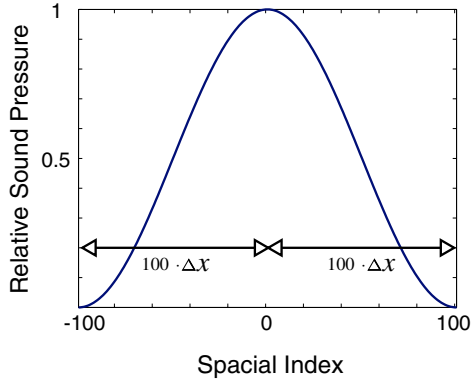


**Fig. 5** Image of source distribution calculated using Eq. (15).

of time period, which satisfies the stability condition as

$$F_s = 2\sqrt{2} \cdot c / \Delta x, \quad (14)$$

where  $F_s$  is the sampling frequency,  $c$  is the sound speed, and  $\Delta x$  is the grid width.

As an initial condition, an impulse source is assumed in a time domain. In a spacial domain, the distribution of sound pressure is set to be

$$p(r) = \begin{cases} 0.5 + 0.5 \cdot \cos(\pi r/R) & \text{if } r \leq R, \\ 0 & \text{if } r > R, \end{cases} \quad (15)$$

where  $r$  is the distance from the center position of the sound source and  $R$  is the radius of the sound source. Figure 5 shows the condition of the sound source in this calculation in which  $R = 100 \cdot \Delta x$ . Using this condition, the absorbed boundary condition is not set; however, a large calculation field is assumed to equivalently realize an infinite field. Figure 6 shows the waveform of the observed sound pressure. The incident and reflected waves are completely separated, as in the case in which an ideal absorbed boundary condition is assumed. The normal incident absorption coefficient  $\alpha_0(\omega)$  is calculated as

$$\alpha_0(\omega) = 1 - \left| \frac{P_{\text{ref}}(\omega)}{P_{\text{inc}}(\omega)} \right|^2, \quad (16)$$

where  $P_{\text{inc}}(\omega)$  and  $P_{\text{ref}}(\omega)$  are the frequency responses of the incident and reflected waves, respectively. They are obtained by the Fourier transform of truncated waves, as

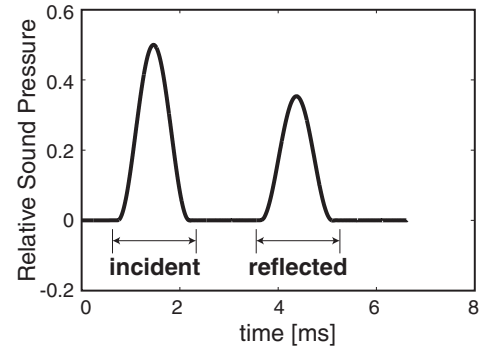


**Fig. 6** Calculated waveform at receiver. The incident wave is separated from the reflected wave. The relative sound pressure is normalized using the initial amplitude of source.

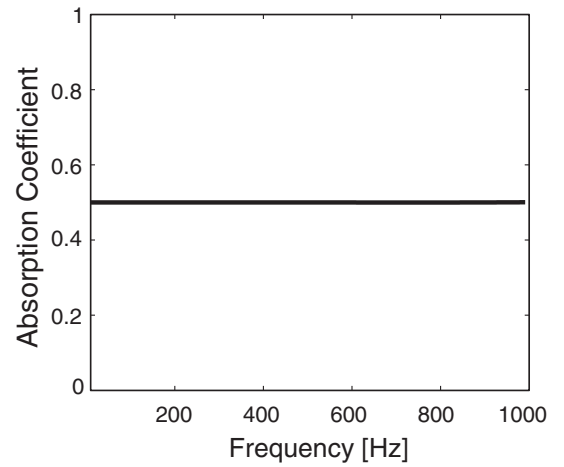


**Fig. 7** Normal incident absorption coefficient calculated from spectra of incident and reflected waves shown in Fig. 6. The expected value is 0.5 at all frequencies, and the result of the simulation is the desired value.

shown in Fig. 6. The conditions assumed are the density  $\rho_2 = 7.0524 \text{ kg/m}^3$  and the sound speed  $c_2 = 343 \text{ m/s}$  in the material. The normal incident absorption coefficient, which is calculated from the waveforms in Fig. 6, should be 0.5 under this condition with an exact solution given by Eq. (8). Figure 7 shows that the normal incident absorption coefficient is equal to 0.5 at all frequencies.

Another calculation is carried out by varying the sound speed in the material. Figure 8 shows the results of this calculation, in which the material mass density  $\rho_2$  is fixed to be  $20 \text{ kg/m}^3$  and the sound speed  $c_2$  is varied to 43, 143, 243, and 343 m/s. All the results are determined by the same procedure as that used in Fig. 7, i.e., by comparing of the incident wave spectrum with the reflected wave spectrum. It is observed that the normal incident absorption coefficients correspond to exact solutions. These results suggest that it is possible to consider various conditions, including the lower sound speed in the material than in air

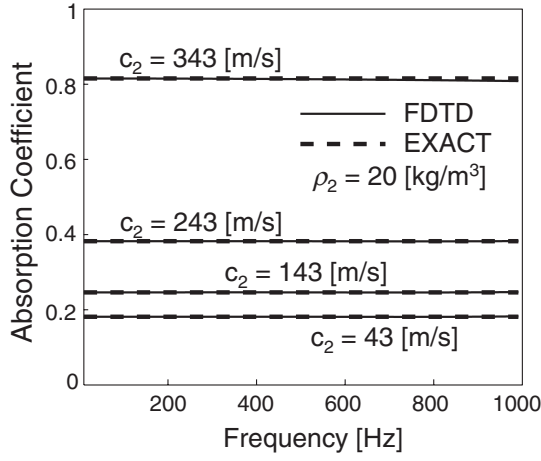


**Fig. 8** Normal incident absorption coefficients obtained by FDTD (solid line) and using exact solution given by Eq. (8) (broken line). The material sound speed in material  $c_2$  is varied with the fixed mass density  $\rho_2 = 20 \text{ kg/m}^3$ .

in this method; that is, locally reactive conditions can be examined.

#### 4. EXAMINATION OF ACCURACY OF METHOD II BASED ON RAYLEIGH MODEL

##### 4.1. Material of Infinite Length

To confirm the accuracy of the Rayleigh model, a one-dimensional tube is assumed, as shown in Fig. 9, and the calculation of sound pressure is carried out by a one-dimensional FDTD method. The normal absorption coefficient is calculated and compared with the exact solution. The conditions used are as follows: a spacing grid of 0.0025 m, a sampling frequency of 388,060 Hz, a porosity of 1, and a flow resistance of  $15,000 \text{ kgm}^{-3} \text{ s}^{-1}$ . The sampling frequency of 388,060 Hz is determined using Eq. (14). In air, sound pressure is updated by using Eqs. (3) and (4). In the material, Eqs. (3) and (13) are used. The sound source and infinite field used are the same as those in Sect. 3.1.

Figure 10 shows the waveform of sound pressure at the receiver and that the incident and reflected waves can be

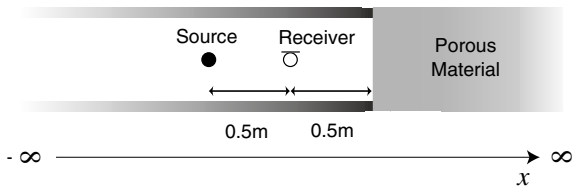


**Fig. 9** Image of one-dimensional sound field used in examination of Rayleigh model, in which acoustic tube of infinite length and porous material of infinite thickness are assumed.

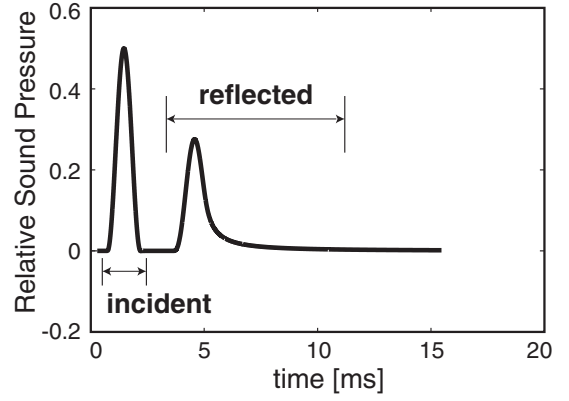


**Fig. 10** Calculated waveform at receiver in Rayleigh model. The relative sound pressure is normalized using the initial amplitude of source.

separated. In this case, it is possible to assume that the material has an infinite thickness. The material characteristic impedance  $Z_{m0}$  is expressed as [3]

$$Z_{m0} = \rho_0 c \left( 1 - \frac{i\mathcal{E}}{\rho_0 \omega} \right)^{\frac{1}{2}}, \quad (17)$$

where  $\mathcal{E}$  is the flow resistance. The normal incident sound absorption coefficient  $\alpha_0$  is calculated as

$$\alpha_0 = 1 - \left| \frac{Z_{m0} - Z_{a0}}{Z_{m0} + Z_{a0}} \right|^2, \quad (18)$$

where  $Z_{a0}$  is the characteristic impedance of air.

Figure 11 shows the calculated result with the exact solution of the normal incident absorption coefficient. The calculated result is similar to the exact solution.

##### 4.2. Material of Finite Thickness

Figure 12 shows a one-dimensional pipe and a material

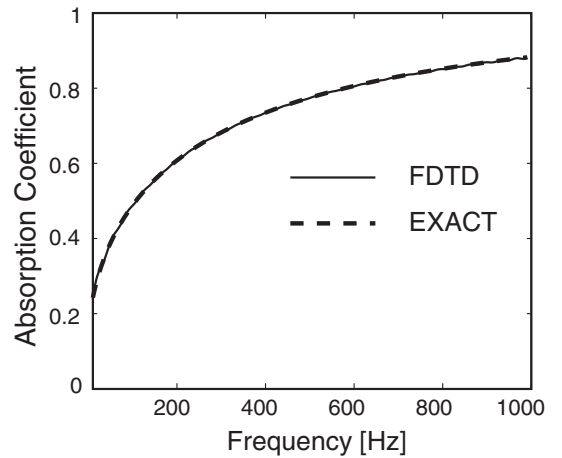


**Fig. 11** Normal incident absorption coefficient obtained by FDTD method with Rayleigh model (solid line) and using exact solution given by Eq. (18) (broken line).

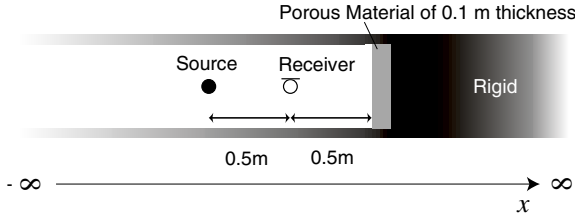


**Fig. 12** Image of one-dimensional sound field used in examination of Rayleigh model, in which acoustic tube of infinite length and porous material of finite thickness with rigid back are assumed.

with a rigid back. The calculation conditions used are as follows: a spacing grid width of 0.0025 m, a sampling frequency of 388,060 Hz, a porosity of 1, a flow resistance of  $15,000 \text{ kgm}^{-3} \text{ s}^{-1}$ , and a material thickness of 0.1 m. The sampling frequency of 388,060 Hz is determined using Eq. (14). The sound source and infinite field used are the same as those in Sect. 3.1. The characteristic impedance  $Z_{m1}$  of the material with a rigid back is expressed as [3]

$$Z_{m1} = -iZ_{m0} \cot \left[ d \frac{\omega}{c} \left( 1 - \frac{i\varepsilon}{\rho_0 \omega} \right)^{\frac{1}{2}} \right], \quad (19)$$

where  $d$  is the thickness of the material and  $Z_{m0}$  is the same as Eq. (17). It is assumed that the rigid back in the FDTD method is realized by setting the particle velocities to be zero on the grids.

Figure 13 shows the result of comparing the normal incident absorption coefficient and exact solution. The normal incident absorption coefficient, which is calculated by the FDTD method, corresponds to the exact solution.

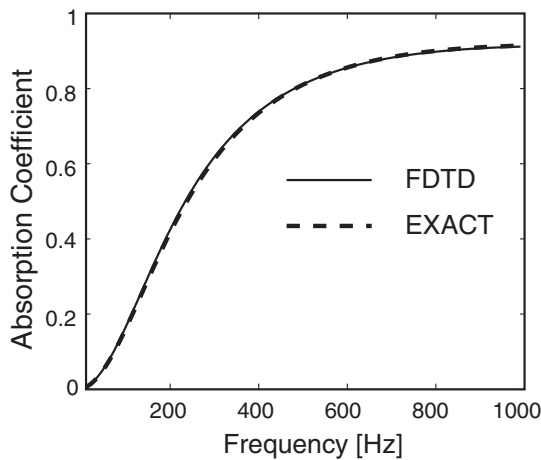


**Fig. 13** Normal incident absorption coefficient obtained by FDTD method with Rayleigh model (solid line) and using the exact solution given by Eq. (19) (broken line).

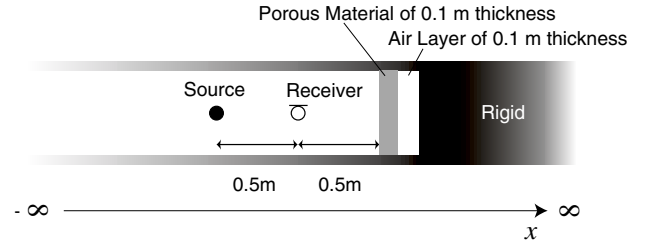


**Fig. 14** Image of one-dimensional sound field used in examination of Rayleigh model, in which acoustic tube of infinite length and porous material of finite thickness with air layer and rigid back are assumed.

### 4.3. Material of Finite Thickness with Air Layer at Its Back

Figure 14 shows another calculation model. The one-dimensional pipe with the material with an air layer at its back is simulated by a one-dimensional FDTD method. The calculation conditions used are as follows: a spacing grid of 0.0025 m, a sampling frequency of 388,060 Hz, a porosity of 1, a flow resistance of  $15,000 \text{ kgm}^{-3} \text{ s}^{-1}$ , and material and air layer thickness of 0.1 m. The sound source and infinite field used are the same as those in Sect. 3.1. The characteristic impedance of the air layer ( $Z_{a1}$ ) with a thickness of  $d$  [m] is expressed as [8]

$$Z_{a1} = -iZ_{a0} \cot(kd), \quad (20)$$

where  $d$  is the thickness of the material and  $Z_{a0}$  is the characteristic impedance of air. The characteristic impedance of the material with the thickness  $d$  [m] thickness is given by Eq. (19). The total characteristic impedance  $Z$  is written as [8]

$$Z = \frac{-iZ_{a1}Z_{m1} + Z_{m0}^2}{Z_{a1} - Z_{m1}}, \quad (21)$$

where  $Z_{m1}$  is the same as Eq. (19). Finally, the normal incident sound absorption coefficient  $\alpha_1$  is calculated as

$$\alpha_1 = 1 - \left| \frac{Z - Z_{a0}}{Z + Z_{a0}} \right|^2. \quad (22)$$

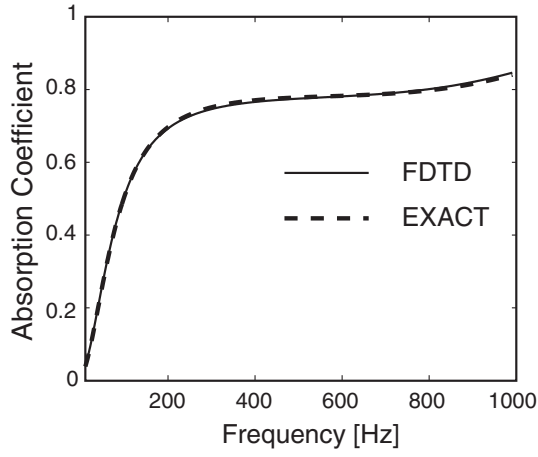
where  $Z_{a0}$  is the characteristic impedance of air. Figure 15 shows the normal incident absorption coefficient. The numerical absorption coefficient corresponds to the exact solution.

## 5. NUMERICAL EXAMPLE IN TWO-DIMENSIONAL SOUND FIELD

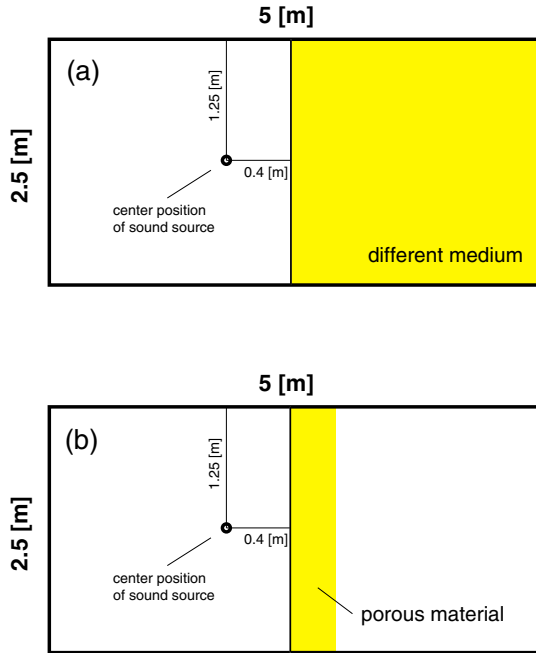
### 5.1. Method I: Varying Sound Speed and Medium Density

Figure 16(a) shows a two-dimensional sound field enclosed by a rigid boundary and two different mediums. A spacial grid width of 0.05 m and a sampling frequency of 19,403 Hz are assumed. This sampling frequency is





**Fig. 15** Normal incident absorption coefficient obtained by FDTD method with Rayleigh model (solid line) and using exact solution given by Eq. (21) (broken line).



**Fig. 16** Image of two-dimensional sound field enclosed by rigid boundary. The left-hand side is filled with air, and the right-hand side is filled with a different medium in (a), and the porous material of finite thickness is arranged at the center in (b).

determined by using Eq. (14). The left-hand side of the field is filled with air, and the right-hand side shows the material with a high density and various sound speeds. The sound source is calculated by using Eq. (15), and the source radius  $2R$  is the eleven grid width, as shown in Fig. 17. Figure 18 shows the results obtained at a density of  $6.05 \text{ kg/m}^3$  and a sound speed of  $343 \text{ m/s}$ . The reflection wave on the left-hand side and the transmitted wave on the right-hand side are shown. Figure 19 shows the results obtained at a density of  $60.5 \text{ kg/m}^3$  and a sound speed of

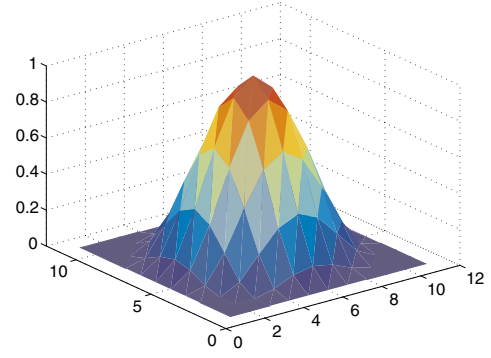


**Fig. 17** Image of source distribution given by Eq. (15).

$34.3 \text{ m/s}$ . The characteristic impedances of the materials assumed in Figs. 18 and 19 are identical. However, in the case in Fig. 19, the sound speed is low, and the transmitted wave on the right-hand side diverges very slowly from that in Fig. 18.

## 5.2. Method II: Rayleigh Model

The Rayleigh model makes it possible to calculate sound fields with porous materials of various sizes and conditions. Figure 16(b) shows the simulated sound field with a porous material with a large air layer at its back. The calculation conditions used are as follows: a grid width of  $0.05 \text{ m}$ , a sampling frequency of  $19,403 \text{ Hz}$ , a flow resistance of  $8,000 \text{ kgm}^{-3} \text{ s}^{-1}$ , and a material thickness of  $0.1 \text{ m}$ . The sampling frequency of  $19,403 \text{ Hz}$  is determined by using Eq. (14). The source condition is the same as the previous condition. Figure 20 shows the changes in calculated field. It is observed that the reflected wave has a complex pattern and that the transmitted wave is moderately attenuated.

Since a practical material does not have uniform characteristics, we have tried to consider such a random variation. Inside the material, we set the mass density  $\rho$  to be  $1.21 \text{ kg/m}^3 \pm 25\%$ , the sound speed  $c$  to be  $343 \text{ m/s} \pm 25\%$  and the flow resistances  $\sigma_x$  and  $\sigma_y$  to be  $8,000 \text{ kgm}^{-3} \text{ s}^{-1} \pm 25\%$ . Inside the material, all properties of each grid are calculated as

$$\rho = 1.21 \cdot (1 + 0.25 \cdot N), \quad (23)$$

$$c = 343 \cdot (1 + 0.25 \cdot N), \quad (24)$$

$$\sigma_x = 8000 \cdot (1 + 0.25 \cdot N), \quad (25)$$

$$\sigma_y = 8000 \cdot (1 + 0.25 \cdot N) \quad (26)$$

where  $N$  is the random value calculated for each grid and the range of this value is from  $-1$  to  $1$ . Figure 21 shows the calculated field with the randomized conditions. It is observed that the reflect wave is dissymmetric because of the randomized medium. This method enables us to examine cases in which the target material has a large



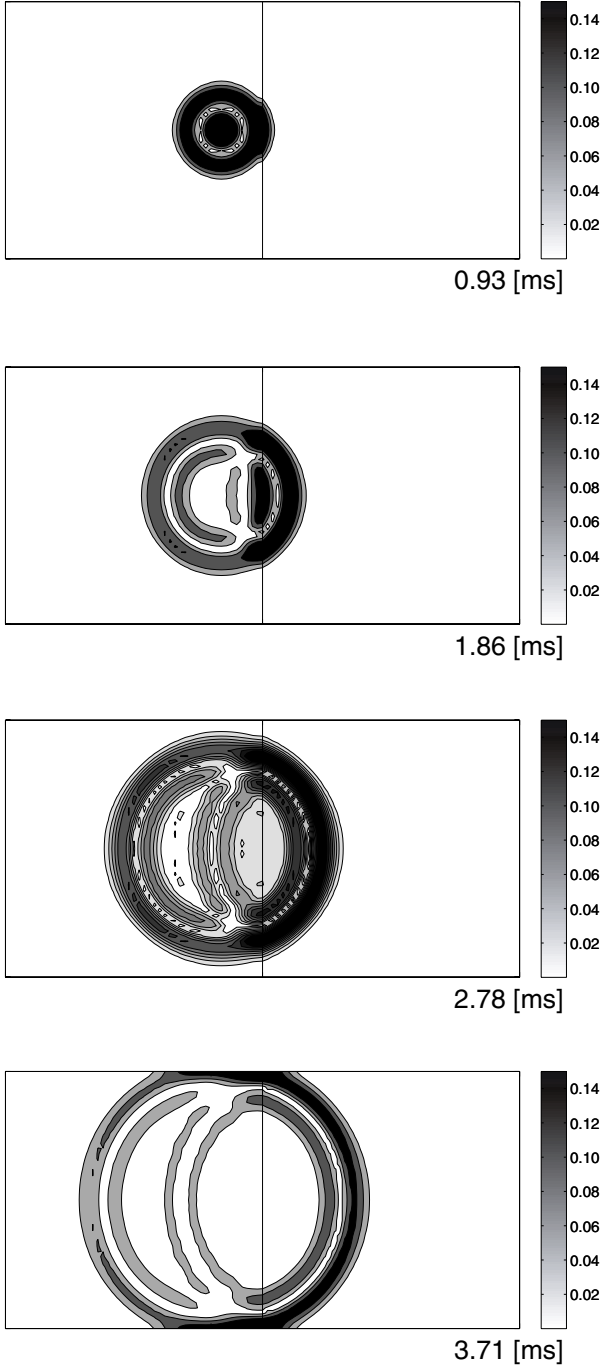


**Fig. 18** Changes in the absolute relative sound pressure distribution on linear scale. The relative sound pressure is normalized using the initial amplitude of the source. A mass density of  $6.05 \text{ kg/m}^3$  and a sound speed of  $343 \text{ m/s}$  are assumed in the right-hand side medium.

distribution of properties, such as sound speed and flow resistance. In this example, the calculation is stable, but general stability conditions should be discussed in a future study.

## 6. CONCLUSION

In this paper, we propose a method that considers

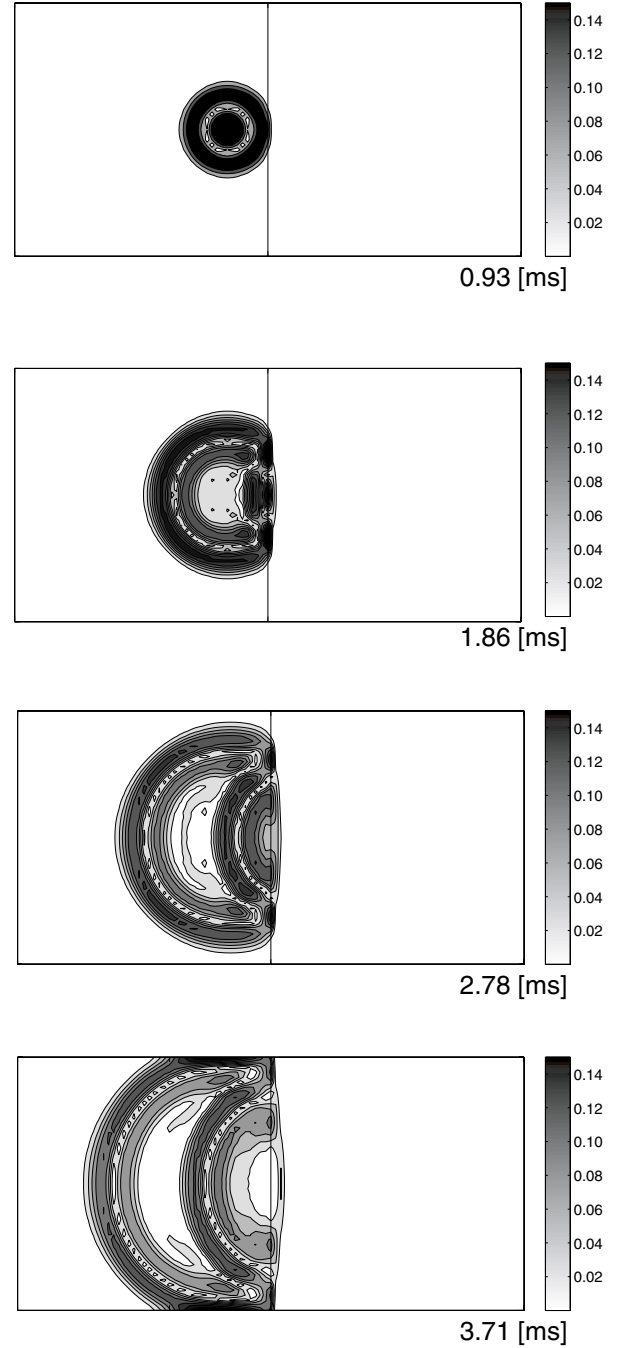


**Fig. 19** Changes in absolute relative sound pressure distribution on linear scale. The relative sound pressure is normalized using the initial amplitude of the source. A mass density of  $60.5 \text{ kg/m}^3$  and a sound speed of  $34.3 \text{ m/s}$  are assumed in the right-hand side medium.

boundary conditions by changing density, sound speed, and flow resistance in an FDTD scheme. A model for the changes in density and sound speed suggests the possibility of considering the various conditions. Another model, which is an extended Rayleigh model, makes it possible to analyze a sound field with a porous material of finite size. Both models show good correspondence with exact solutions and have large advantages in that practical coding is

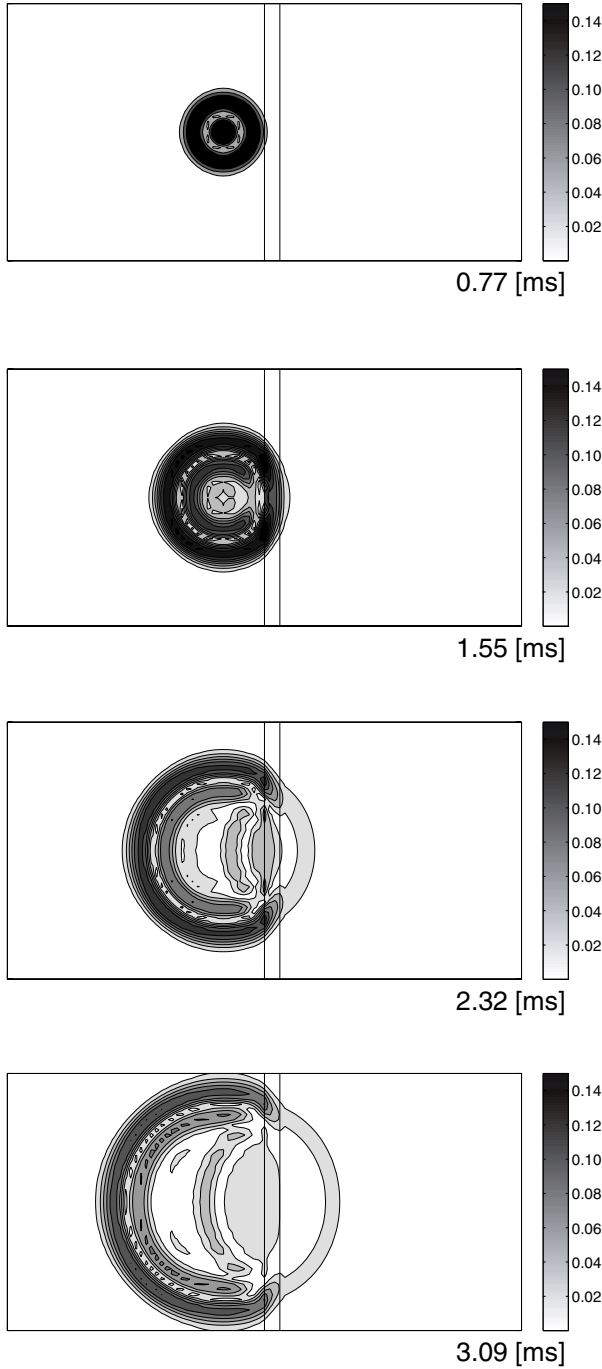


**Fig. 20** Changes in absolute relative sound pressure distribution on linear scale. The relative sound pressure is normalized using the initial amplitude of the source. A mass density of  $1.21 \text{ kg/m}^3$  and a sound speed of  $343 \text{ m/s}$  in the air layer, and a flow resistance of  $8,000 \text{ kgm}^{-3} \text{ s}^{-1}$  for a  $0.1\text{-m}$ -thick porous material are assumed.

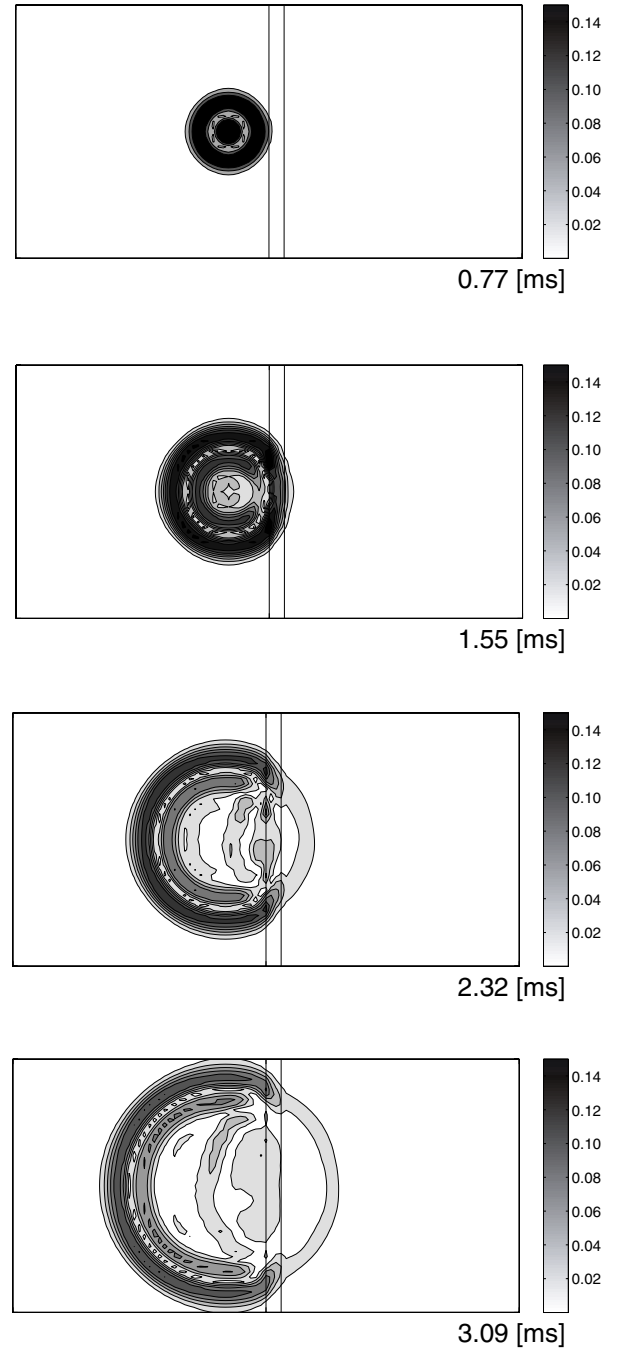


**Fig. 21** Changes in absolute relative sound pressure distribution on linear scale. The relative sound pressure is normalized using the initial amplitude of the source. A mass density of  $1.21 \text{ kg/m}^3 \pm 25\%$  and a sound speed of  $343 \text{ m/s} \pm 25\%$  in the air layer, and a flow resistance of  $8,000 \text{ kgm}^{-3} \text{ s}^{-1} \pm 25\%$  for a  $0.1\text{-m}$ -thick porous material are assumed.

## REFERENCES

very easy and is realized by slightly modifying of the pre-existing code.

As future work, a comparisons of models, such as Delany-Bazley and Miki models should be considered. Moreover, the examination of experimental results obtained under various conditions should be carried out.

- [1] O. Chiba and T. Kashiwa, "Analysis of sound fields in three dimensional space by the time-dependent finite-difference method based on the leap frog algorithm," *J. Acoust. Soc. Jpn. (J)*, **49**, 551–562 (1993).
- [2] T. Yokota, S. Sakamoto and H. Tachibana, "Visualization of sound propagation and scattering in rooms," *Acoust. Sci. & Tech.*, **23**, 40–46 (2002).

- [3] H. Kuttruff, *Room Acoustics* (Elsevier Applied Science, Essex, 2000), pp. 150–161.
- [4] S. Sakamoto, Y. Tokita and H. Tachibana, “Calculation of impulse responses of rooms by using of the finite difference method,” *Proc. 3rd ASA/ASJ Jt. Meet.*, pp. 1307–1310 (1996).
- [5] M. E. Delany and E. N. Bazley, “Acoustical properties of fibrous absorbent materials,” *Appl. Acoust.*, **3**, 105–116 (1970).
- [6] Y. Miki, “Acoustical properties of porous materials –Modifications of Delany-Bazley models–,” *J. Acoust. Soc. Jpn. (E)*, **11**, 19–24 (1990).
- [7] D. Botteldooren, “Acoustical finite-difference time-domain simulation in a quasi-Cartesian grid,” *J. Acoust. Soc. Am.*, **95**, 2313–2319 (1994).
- [8] T. J. Cox and P. D’Antonio, *Acoustic Absorbers and Diffusers* (Spon Press, London, 2004), pp. 148–150.

**Hisaharu Suzuki** was born in Nara, Japan, 1979. He received B. Design and M. Design degrees from Kyushu Institute of Design in 1998 and 2004, respectively. He is currently working toward the Ph. D degree at Kyushu University. His current research interests include active control of energy flow and modeling of acoustic material. He

has two freeware projects for calculating and measuring sound field at <http://foac.nomoo.info> and <http://opam.nomoo.info>.

**Akira Omoto** graduated from the Kyushu Institute of Design, Fukuoka Japan, in 1987, and received the Dr. Eng. degree from the University of Tokyo, Japan, in 1995. From 1987 to 1991, he worked at Nittobo Acoustic Engineering Co., Ltd., Tokyo. In 1991, he was appointed Research Associate at Kyushu Institute of Design, and was made Associate Professor in 1997. His current research interests include measurement, evaluation and control of the small sized enclosure.

**Kyoji Fujiwara** graduated from Kobe University in 1969, and received M. E. degree from Kobe University in 1971. He received Dr. Eng. degree from the University of Tokyo in 1979. He began to work as a Research Associate at the Department of Acoustic Design, Kyushu Institute of Design from 1971, and was promoted to Associate Professor in 1985. Since 1989, he is Full Professor. He is now a member of Acoust. Soc. Jpn., Acoust. Soc. Am, Architectural Inst. of Jpn. and INCE/Japan.